

Mechanical properties of ultrafine grained ferritic steel sheets fabricated by rolling and annealing of duplex microstructure

Yoshitaka Okitsu · Naoki Takata · Nobuhiro Tsuji

Received: 6 March 2008 / Accepted: 26 August 2008 / Published online: 18 September 2008
© Springer Science+Business Media, LLC 2008

Abstract A new route to fabricate ultrafine grained (UFG) ferritic steel sheets without severe plastic deformation is proposed in this article. A low-carbon steel sheet with a duplex microstructure composed of ferrite and martensite was cold-rolled to a reduction of 91% in thickness, and then annealed at 620–700 °C. The microstructure obtained through the process with annealing temperatures below 700 °C was the UFG ferrite including fine cementite particles homogenously dispersed. The grain size of ferrite matrix changed from 0.49 to 1.0 μm depending on the annealing temperature. Dynamic tensile properties of the produced UFG steels were investigated. The obtained UFG ferrite–cementite steels without martensite phase showed high strain rate sensitivity in flow stress. The UFG ferritic steels are expected to have high potential to absorb crash energy when applied to automobile body.

Introduction

Ultrafine grained (UFG) steels with grain size smaller than a few micrometer are expected to be new structural materials, because of their superior mechanical properties such as high strength [1], good fracture toughness at low temperature [2], high dynamic strength (strength at very high strain rate around 10^3 s^{-1}) [3, 4]. Especially dynamic deformation properties are important if the UFG steels are considered as materials for automobile body applications. Up to now, however, it has been difficult to apply the UFG steel sheets to automobile body parts, because of the limited dimensions of samples fabricated by severe plastic deformation (SPD) processes such as equal channel angular extrusion [5, 6], high pressure torsion [7], and ARB [1]. Also the SPD processes do not seem to be adaptive to the conventional mass production routes for steels.

The authors of this article have achieved to fabricate the bulky UFG steel sheets through conventional rolling and annealing procedures without SPD. The proposed process is characterized by the starting microstructure, which is a dual phase microstructure composed of ferrite and martensite. In the present study, the microstructures obtained by the new process are shown and the mechanism of microstructure evolution is discussed. The mechanical properties including dynamic tensile properties of the fabricated UFG steels are also shown and discussed.

Experimental

The chemical composition of the steel studied is listed in Table 1. The transformation temperatures on cooling from austenite, which were important for fabricating the dual phase starting microstructure, were measured by a

Y. Okitsu (✉)
Automobile R&D Center, Honda R&D, Co., Ltd.,
4630 Shimotakanezawa, Haga-machi, Haga-gun,
Tochigi 321-3393, Japan
e-mail: yoshitaka_okitsu@n.t.rd.honda.co.jp

N. Takata
Department of Metallurgy and Ceramics Science,
Graduate School of Science and Engineering,
Tokyo Institute of Technology, 2-12-1-S8-8 Ookayama,
Meguro-ku, Tokyo 152-8552, Japan
e-mail: ntakata@mtl.titech.ac.jp

N. Tsuji
Department of Adaptive Machine Systems,
Graduate School of Engineering, Osaka University,
2-1 Yamadaoka, Suita, Osaka 565-0871, Japan
e-mail: tsuji@ams.eng.osaka-u.ac.jp

Table 1 Chemical composition of the steel studied (mass%)

C	Si	Mn	P	S	Al	Nb	B	N
0.10	0.01	1.98	0.002	0.001	0.018	0.018	0.0015	0.0011

dilatometer. The two-phase region of ferrite and austenite at cooling rate of $2\text{ }^{\circ}\text{C s}^{-1}$ was clarified to be between 465 and 625 $^{\circ}\text{C}$.

An ingot of the steel was heated and hot-rolled to the thickness of 6.8 mm at austenite region. After the hot-rolling, the sheet was air-cooled to 540 $^{\circ}\text{C}$, which corresponds to the intercritical region of ferrite and austenite, and then immediately cooled by water spray to room temperature for fabricating a dual phase microstructure of ferrite and martensite. The hot-rolled sheets were cold-rolled at room temperature using a four-high rolling mill with lubricant. Cold-rolled sheets having 150 mm width and 0.6 mm thickness were obtained. The total reduction in thickness through the cold-rolling was 91%, corresponding to an equivalent plastic strain of 2.8. The cold-rolled sheets were annealed at various temperatures ranging from 620 to 700 $^{\circ}\text{C}$ in a salt bath followed by water-cooling.

Microstructural observations were carried out for the specimens at each stage of the process. All specimens were observed from the transverse direction (TD) of the sheets. The samples for optical microscope or scanning electron microscope (SEM) were etched with a 3% nital. SEM observations were conducted on Hitachi S-4300E/N SEM operated at 15 kV. Thin foils for transmission electron microscope (TEM) were prepared by twin-jet electropolishing in a 10% $\text{HClO}_4 + 90\% \text{CH}_3\text{COOH}$ solution, and observed with JEOL JEM-2010HC TEM operated at 200 kV. An electron backscatter diffraction (EBSD) analysis was also carried out by using FEI XL30S SEM equipped with TSL (TexSEM Laboratories, Inc.) orientation image microscope system operated at 15 kV. The EBSD scanning was carried out at the center of thickness on the TD section. The mapping was carried out at a step size of 0.05 or 0.1 μm on a hexagonal grid.

Quasi-static and dynamic tensile properties were investigated by using a load sensing block [8, 9] type high-speed material test system (TS-2000) [10]. Tensile specimens with a gauge length of 6 mm and a width of 2 mm, of which tensile direction was parallel to RD, were prepared, and tested at various strain rates ranging from 10^{-2} to 10^3 s^{-1} at room temperature.

Results and discussion

Microstructures of hot-rolled and cold-rolled specimens

An optical micrograph of the hot-rolled steel sheet observed from TD is shown in Fig. 1. The hot-rolled sheet

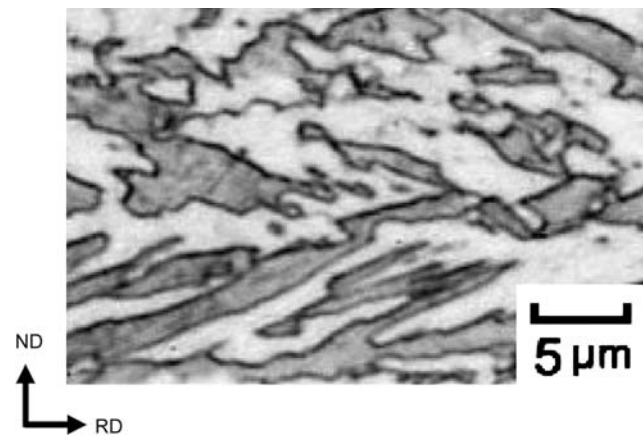


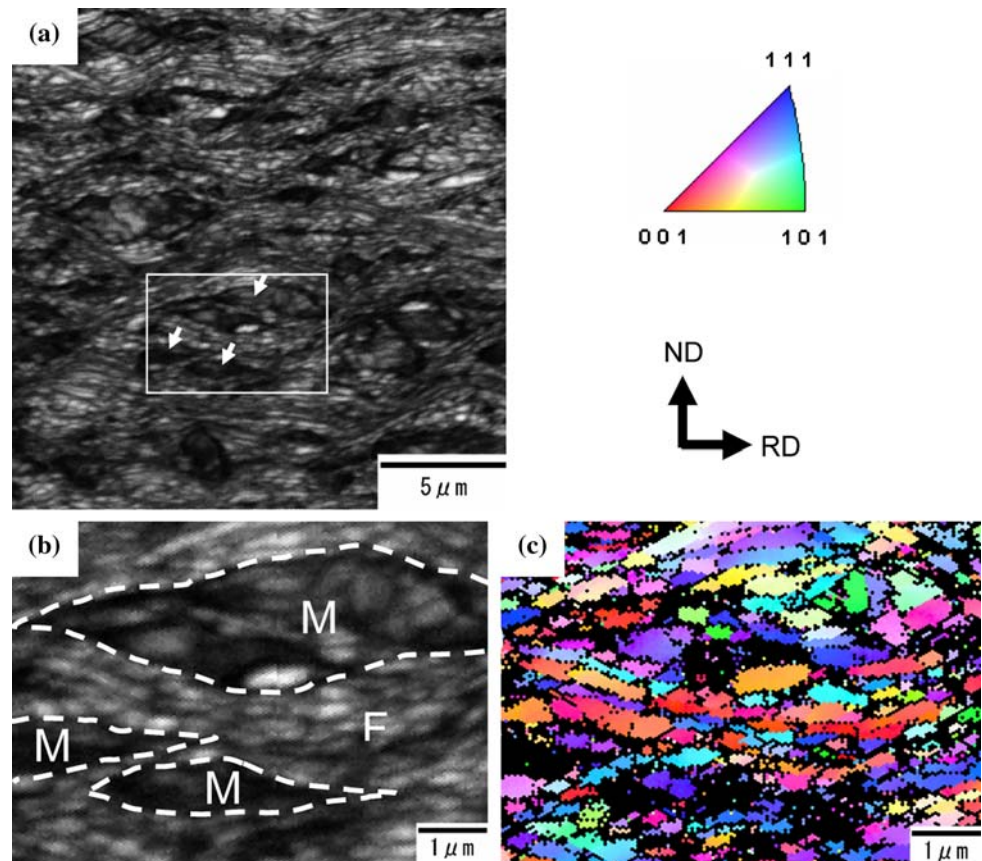
Fig. 1 Optical micrograph of the 0.1C–2Mn steel hot-rolled sheet before cold-rolling. Observed from TD

showed a duplex microstructure composed of ferrite matrix (bright region in Fig. 1) and martensite (dark region in Fig. 1). The area fraction of martensite was 42%. The TEM observation confirmed that the martensite was “lath-martensite” including high density of dislocations. Cementite particles were not observed.

The microstructure of the cold-rolled specimen was investigated by SEM and EBSD analysis. Figure 2a shows an image quality (IQ) map obtained by the EBSD measurement for a $20 \times 20\text{ }\mu\text{m}^2$ area on TD section of the 91% cold-rolled specimen. The ferrite matrix (bright region) and martensite (dark region) are recognized. Martensite regions are indicated by white arrows in Fig. 2a. Figure 2b shows an enlarged IQ map of the rectangular area with a size of $5 \times 7\text{ }\mu\text{m}^2$ in Fig. 2a. The “F” and “M” in the figure indicate ferrite and martensite, respectively. The boundaries between ferrite and martensite are indicated by dashed white lines. Figure 2c shows an ND orientation color map of the same area as Fig. 2b. The measured pixels of which confidence index (CI) values are smaller than 0.1 are colored in black, because the orientation analysis was not accurate in those pixels. The ferrite matrix exhibits wavy microstructure elongated roughly to RD and bent along martensite islands. It is suggested that complex plastic flow occurred and high strain was introduced in the ferrite matrix owing to the existence of the hard martensite phase. A lamellar structure of ferrite with mean spacing of 0.22 μm was observed in Fig. 2b. The lamellar structure contained ultrafine grains with large misorientations, as is indicated by various colors in Fig. 2c. The results indicate that a kind of UFG microstructure in ferrite matrix was already achieved in the cold-rolled state.

It is well known that the hard second particles increase the rate of formation of high angle grain boundaries (HAGBs) in the matrix through heavy deformation in two-phase metals [11]. It is caused by local lattice rotations in

Fig. 2 Orientation imaging microstructures obtained by EBSD measurement of the low-carbon steel cold-rolled by 91% reduction. Observed from TD. (a) IQ map of a large area. White arrows indicate martensite. (b) Enlarged IQ map of the rectangular area in (a). F and M indicate ferrite and martensite, respectively. (c) Orientation color map of the same area as (b). The measured pixels having the CI smaller than 0.1 are colored in black



the vicinity of the hard particles. In the present study, the formation of HAGBs in ferrite matrix was probably accelerated by hard martensite phase. In addition, shear strain should be closely related to the significant grain refinement of ferrite matrix. Kamikawa et al. [12] have reported that redundant shear strain accelerates the microstructure refinement through the ARB in interstitial free (IF) steel. The wavy-shaped ferrite and diamond-shaped martensite shown in Fig. 2a suggest that severe shear strain was introduced, so that the formation of HAGBs associated with lattice rotation was accelerated.

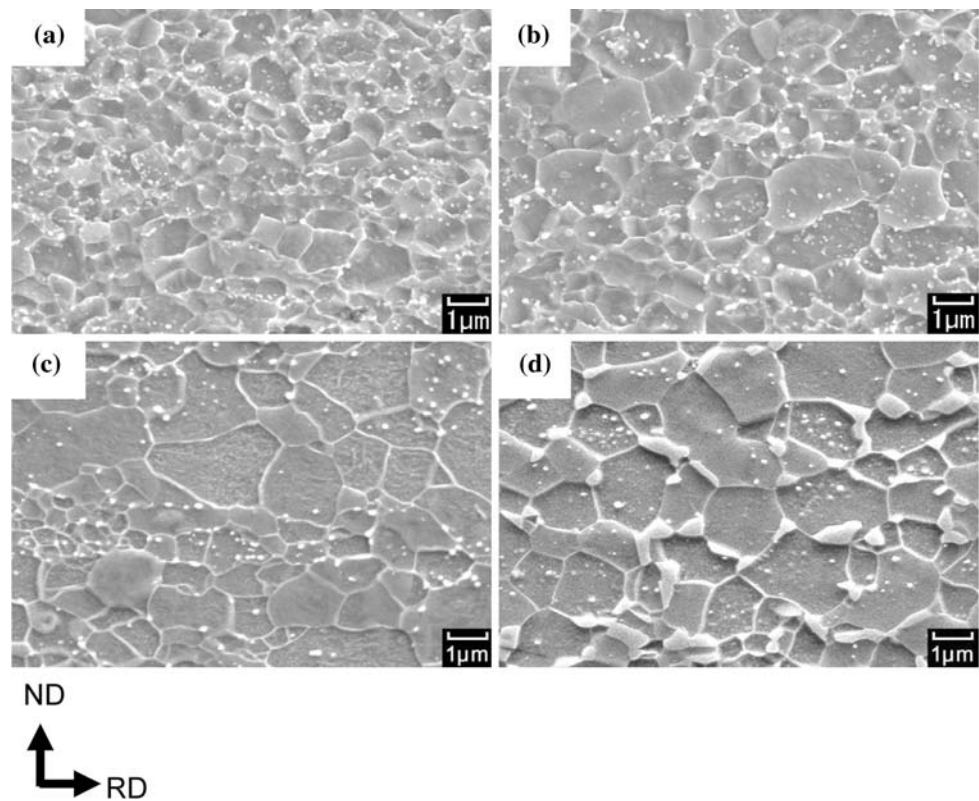
On the other hand, as shown in Fig. 2a and b, the martensite regions having diamond shapes were also deformed to some extent in cold-rolling. The strain introduced into martensite should be smaller than that into ferrite matrix, because martensite is much harder than ferrite. Nevertheless, the martensite was also subdivided into fine regions surrounded by high-angle boundaries, as shown in Fig. 2c. It has been reported that 50% cold-rolled low-carbon martensite exhibited fine lamellar structure involving large misorientations [13]. Similar ultrafine lamellar structure has been also reported in an 80% cold-rolled martensite of an ultra-low carbon IF steel [14]. Those results have been thought to be attributed to the complicated and fine microstructure of the as-quenched

martensite including high density of dislocations. It can be concluded therefore that the strain introduced to martensite was not very large but probably enough to subdivide the microstructure finely.

Microstructures of annealed specimens

Figure 3a–d shows SEM images of the specimens after annealing at 620, 635, 655, and 700 °C, respectively. They were observed from TD. The cold-rolled microstructure changed to equiaxed UFG ferrite grains including fine cementite particles during the annealing at the temperature below 700 °C. The cementite particles were homogeneously dispersed within the UFG ferrite matrix. The ferrite grain size increased with increasing annealing temperature. When annealed at 700 °C, a complex microstructure composed of fine ferrite matrix, cementite (white fine particles), and martensite (lightly etched islands on grain boundaries and grain boundary triple junctions) formed. The dilatometer measurement revealed that A_1 transformation temperature on heating was approximately 700 °C, which meant that cementite partly resolved to ferrite matrix, austenite phase appeared during annealing at 700 °C, and then the austenite transformed to martensite during water-cooling. The EBSD analysis revealed that the

Fig. 3 SEM images of the low-carbon steel cold-rolled by 91% reduction, annealed at (a) 620 °C, (b) 635 °C, (c) 655 °C, and (d) 700 °C for 120 s and water cooled to room temperature



fractions of HAGBs of which misorientations are higher than 15° in the annealed specimens shown in Fig. 3a–d were 77.4, 85.4, 85.1, and 87.5%, respectively. It was also found that the fraction of HAGBs in the specimen annealed at 680 °C, that showed similar microstructure to Fig. 3a–c, was 90.1%. It is, therefore, confirmed that the ultrafine ferrite grains obtained by the present process have large misorientation to each other. The fraction of HAGBs increased with increasing annealing temperature, which suggests that some low-angle grain boundaries were annihilated in annealing.

Figure 4 shows the distributions of grain diameter obtained by the EBSD analysis of the annealed specimens. As the grain diameter of each grain, the diameter of a circle having the same area as the measured grain was used. The distributions of the grain diameter were rather broad. For example, some coarse grains larger than 2 μm existed in the specimen annealed at 620 °C, but the average grain diameter was 0.49 μm. The average grain diameters of ferrite in other annealed specimens shown in Fig. 4b–d were 0.62, 0.85, and 1.0 μm, respectively.

It was shown that the UFG ferrite microstructures including fine cementite particles were produced by cold-rolling and substantial annealing of ferrite–martensite duplex starting microstructure, in spite of rather low equivalent strain (2.8) accumulated through the conventional cold-rolling. It is generally known that extremely

high equivalent strain over 4 or 5 is required for producing the ultrafine microstructure through SPD [15]. The microstructural analysis in the present study revealed that the cold-rolled specimen contained a large amount of HAGBs. In ordinary cold-rolling and annealing, recrystallization nucleus appears and grows consuming the deformed region in annealing. In the present study, however, the grains were already finely subdivided by the deformation-induced HAGBs and continuous coarsening of the finely subdivided regions together with recovery process happened to form the UFG microstructure as shown in Fig. 3.

Tensile properties

Quasi-static mechanical properties of the steel specimens obtained by various annealing conditions measured at a strain rate of 10^{-2} s^{-1} are listed in Table 2. The 0.2% offset stress decreased with the increase in ferrite grain size. The tensile strength also decreased with the increase in ferrite grain size only when the microstructure was ferrite–cementite. On the other hand, the tensile strength of ferrite–cementite–martensite specimen (700 °C annealed) was higher than that of ferrite–cementite specimen with mean ferrite grain size of 0.85 μm, which is attributed to large strain-hardening of the steel caused by hard martensite phase.

In order to investigate the strain rate dependence of the flow stress, the difference in tensile flow stress at 5% strain

Fig. 4 Grain diameter distributions indicated by area fraction in the low-carbon steel cold-rolled by 91% reduction and annealed at (a) 620 °C, (b) 635 °C, (c) 655 °C, and (d) 700 °C for 120 s followed by water-cooling

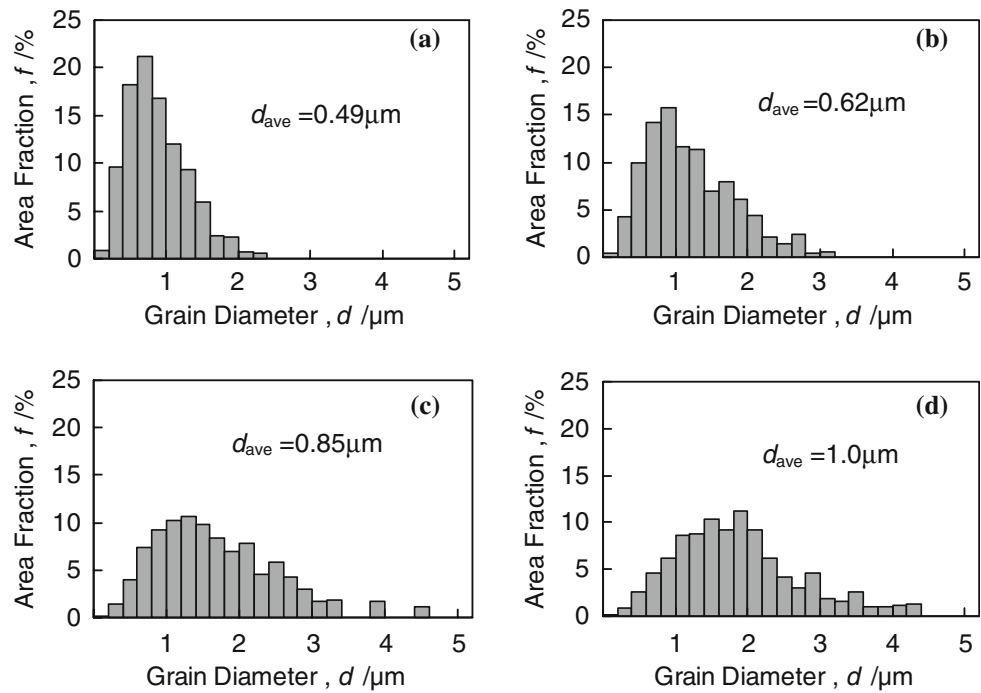


Table 2 Microstructure, ferrite grain size, and mechanical properties of the specimens obtained by various annealing conditions

Annealing condition	Microstructure	Mean ferrite grain size (μm)	0.2% offset stress (MPa)	Tensile strength (MPa)
620 °C, 120 s	F–C	0.49	966	966
635 °C, 120 s	F–C	0.62	816	820
655 °C, 120 s	F–C	0.85	658	672
700 °C, 120 s	F–C–M	1.0	515	753

F, ferrite; C, cementite; M, martensite

Table 3 Microstructure, mean ferrite grain size, and $\Delta\sigma$ of the specimens obtained by various annealing conditions in the present work and several steels reported

Microstructure	Mean ferrite grain size (μm)	$\Delta\sigma$ (MPa)	References
F–C	0.62	161	Present work
F–C	0.85	182	Present work
F–C–M	1.0	63	Present work
F–C	0.7–13.6	167	[18]
F (commercial IF steel)	–	188	[16]
F–M (commercial dual-phase steel)	–	66	[17]

The strains at which $\Delta\sigma$ were measured in references [18], [16], and [17] are 7, 10, and 5–10%, respectively

F, ferrite; C, cementite; M, martensite

between the strain rates of 10^3 and 10^{-2} s^{-1} , $\Delta\sigma$ was evaluated. Measured $\Delta\sigma$ of the UFG ferritic steel specimens of the present work are listed in Table 3, together with reference data of another steel with various microstructures. The $\Delta\sigma$ of the UFG ferrite–cementite specimens in the present work with sub-micrometer grain sizes were as high as that of IF steel [16] with ferrite single phase, but the ferrite–cementite–martensite specimen obtained in the present work showed lower $\Delta\sigma$ (around 60 MPa), which is

close to that of commercial dual-phase steel [17]. It is revealed that the change of microstructure from ferrite–cementite to ferrite–cementite–martensite significantly decreased the $\Delta\sigma$.

The strain rate sensitivity of flow stress is explained in terms of the thermal activated process of the dislocation motion against the Peierls potential. The higher the strain rate is, the higher the external stress is required for the dislocation motion, because the assist by thermal vibration

of atoms decreases. The change in the external stress appears as the strain rate sensitivity of the flow stress. On the other hand, there is another stress component which is independent of strain rate and temperature. The component of flow stress which is related to thermal activation process is called thermal stress, while the other component is called athermal stress. So that, if the thermal stress is decreased by strengthening of steels, the strain rate sensitivity of the flow stress would decrease. It has been reported that grain refinement strengthening mainly contributes to the increase in the athermal stress component which is independent of the strain rate [3, 4], so that the strain rate sensitivity of the flow stress does not change. It means that the steels strengthened by ultra grain refinement keep high strain rate sensitivity that is an essential feature of ferrite (BCC) matrix.

It has already reported that the strain rate sensitivity decreases when the steel is strengthened by the hard second phases [16–18]. Tsuchida et al. [18] explained that the second phases decrease the thermal stress component of the materials. The present result suggests that grain refinement is effective for increasing dynamic strength as well as static strength. The result that the present UFG ferrite–cementite steels have high dynamic strength suggests that they would show good performance for crash energy absorption when applied to the body parts of automobiles.

Conclusions

A new route to fabricate UFG steel sheets through conventional cold-rolling and annealing procedures was shown, and tensile properties of the obtained UFG sheets were investigated. The major results are summarized below.

(1) UFG ferrite–cementite steel sheets with sufficient dimensions (0.6 mm × 150 mm × length) could be produced by conventional cold-rolling and subsequent short-time annealing of dual phase microstructure composed of ferrite and martensite. Only a plastic strain of 2.8 by cold-rolling was enough to obtain the equiaxed UFG ferrite with grain sizes from 0.49 to 1.0 μm throughout the specimen.

(2) The obtained UFG ferrite–cementite steel sheets showed high strain rate sensitivity of the flow stress. It is suggested that UFG ferritic steels have possibility to improve crash energy absorption if it is applied to automobile body parts, compared with conventional high strength steels.

References

1. Tsuji N, Ito Y, Saito Y, Minamino Y (2002) *Scripta Mater* 47:893. doi:10.1016/S1359-6462(02)00282-8
2. Tsuji N, Okuno S, Koizumi Y, Minamino Y (2004) *Mater Trans* 45:2272. doi:10.2320/matertrans.45.2272
3. Jia D, Ramesh KT, Ma E (2003) *Acta Mater* 5:3495. doi:10.1016/S1359-6454(03)00169-1
4. Tsuchida N, Masuda H, Harada Y, Fukaura K, Tomota Y, Nagai K (2008) *Mater Sci Eng A* 488:446. doi:10.1016/j.msea.2007.11.047
5. Segal VM (1995) *Mater Sci Eng A* 197:157. doi:10.1016/0921-5093(95)09705-8
6. Iwahashi Y, Wang J, Horita Z, Nemoto M, Langdon TG (1996) *Scripta Mater* 35:143. doi:10.1016/1359-6462(96)00107-8
7. Valiev RZ, Korznikov AV, Mulyukov RR (1993) *Mater Sci Eng A* 168:141. doi:10.1016/0921-5093(93)90717-S
8. Tanimura S, Mimura K, Umeda T (2003) *J Phys IV* 110:385. doi:10.1051/jp4:20020724
9. Chuman Y, Kimura K, Tanimura S (1997) *Int J Impact Eng* 19:165. doi:10.1016/S0734-743X(96)00019-X
10. Website of Saginomiya Seisakusyo Inc. <http://www.saginomiya.co.jp/eng/dynamic/zairyo/zairyo08.html>. Accessed 22 Aug 2008
11. Humphreys FJ, Hatherly M (2004) *Recrystallization and related annealing phenomena*, 2nd edn. Elsevier, Oxford, p 457
12. Kamikawa N, Sakai T, Tsuji N (2007) *Acta Mater* 55:5873. doi:10.1016/j.actamat.2007.07.002
13. Ueji R, Tsuji N, Minamino Y, Koizumi Y (2002) *Acta Mater* 50:4177. doi:10.1016/S1359-6454(02)00260-4
14. Morito S, Huang X, Furuhashi T, Maki T, Hansen N (2004) *Proceedings of the 25th Riso international symposium on materials science*, p 453
15. Kamikawa N, Tsuji N, Saito Y (2003) *Tetsu-to-Hagane* 89:273 (in Japanese)
16. Takagi S, Tokita Y, Sato K, Shimizu T, Hashiguchi K, Ogawa K et al (2005) *Spec Publ Soc Automot Eng No. SP-1954:7*
17. Takahashi M, Uenishi A, Yoshita H, Kuriyama Y (2003) *Int Body Eng Conf* 2003:7
18. Tsuchida N, Tomota Y, Nagai K (2004) *Tetsu-to-Hagane* 90:1043 (in Japanese)